# A Transient Method for Mass-Transfer Characterization Through Supported Zeolite Membranes: Extension to Two Components

**Lucile Courthial and Arnaud Baudot**
IFP Energies nouvelles, Direction Catalyse et Séparation, Rond-point de l'échangeur de Solaize, BP 3, 69360 Solaize, France

**Mélaz Tayakout-Fayolle**
Université Lyon 1, CNRS, IRCELYON, UMR 5256, Institut de recherches sur la catalyse et l'environnement de Lyon, 2 avenue Albert Einstein, F-69626 Villeurbanne, France

**Christian Jallut**
Université Lyon 1, CNRS, ESCPE, LAGEP, UMR 5007, 43 Bd du 11 Novembre 1918, F-69622 Villeurbanne, France

*DOI 10.1002/aic.13866*
*Published online July 3, 2012 in Wiley Online Library (wileyonlinelibrary.com).*

*In a previous work (Courthial et al.) a transient state characterization method for zeolite supported membranes has been proposed and tested for single components in the Henry domain. An extension of the method to single components beyond the Henry domain and to binary mixtures is described. Since the method is based on experiments performed within the linear domain, the dynamic model previously developed for single components in the Henry domain is extended. The parameter estimation procedure that is described is based on a deep analysis of the model structure with respect to its structural identifiability properties. Some experimental results concerning pure* n-*butane as well as isobutane*/n-*butane mixtures transport through mordenite framework inverted (MFI)-supported membranes are finally shown to illustrate the technique.* © 2012 American Institute of Chemical Engineers *AIChE J,* 59: 959–970, 2013
*Keywords: transient techniques, dynamic modeling, parameter estimation, structural identifiability, membrane, zeolite, mass transfer*

## Introduction

Due to their molecular sieving and host–adsorbate interaction properties, zeolitic materials are often used for the separation of hydrocarbon mixtures. ZSM-5 (pure-silica analog, silicalite-1) or mordenite framework inverted (MFI) is the most widely applied. Due to their pore dimensions (about 0.55 nm), these zeolites are well suited to achieve a shape-selectivity separation of alkane isomers. Thus, supported zeolite membranes, which are made of a continuous (leakage-free) crystal layer deposited on a porous support to ensure mechanical strength, are particularly well adapted to carry out high-temperature alkane isomers' separation. The MFI zeolite layers were synthesized at IFP Energies nouvelles by using the pore-plugging method. The description of their structure and geometry can be found elsewhere[1,2] as well as their synthesis procedure.[3–5]

According to the way they are synthesized, such supported membranes can hardly be properly characterized by nondestructive methods.[6] As an illustration, as the thickness of the zeolitic layer is not well defined, only transient techniques can lead to a complete characterization result of the membrane selective layer.[7] Macroscopic transient techniques are very familiar to people dealing with granular adsorbent materials' characterization through the use of chromatographic[8–13] or temporal analysis of products (TAP) techniques.[14] As far as membranes are concerned, transient techniques are also frequently used. A recent review is available concerning their applications to microporous materials.[7] The main point is to transpose the transient approach as it is applied to granular materials' fixed beds to the geometry of membrane equipments. In the case of supported membranes, the transient version of the Wicke-Kallenbach diffusion cell by using a sweep gas seems to be the most suitable approach.[7] Such an approach based on step changes of the feed composition has been proposed for single components in the case of an embedded single zeolite crystal[15] and in the case of a zeolitic layer grown on a porous sintered stainless steel support.[16] The same method has been applied to tubular supported zeolite membranes.[17–19]

We have also developed an *in situ* nondestructive transient characterization technique[1,2,20,21] by operating the same experimental set-up but according to a completely different way. The zeolitic layer is set at thermodynamic equilibrium by feeding both the inner (retentate) and outer (permeate) compartments by the same mixture at the same pressure.

Correspondence concerning this article should be addressed to C. Jallut at jallut@lagep.univ-lyon1.fr.

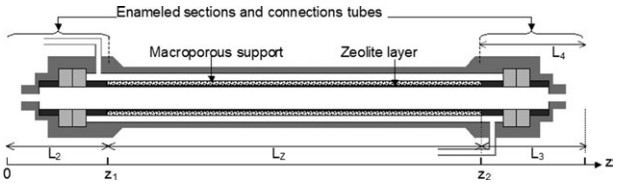


**Figure 1. View of the membrane module.**

A pulse-injection is then applied at the inner compartment inlet instead of a step change and the inner and outer compartments' outlet compositions time evolutions are measured. This approach was inspired by what is commonly achieved by inverse chromatography[10,12] and can be applied for single adsorbates or mixtures. If the concentration pulse intensity is sufficiently low, the behavior of the system is linear and the heat effect of adsorption can be minimized. Operating in the linear domain is strictly necessary as it enables to describe mass transfer through the zeolitic layer according to constant diffusion coefficients Fick's law and linear equilibrium conditions. By superimposing the concentration pulse to the equilibrium baseline, the evolution of the thermodynamic and transport parameters of the zeolitic layer can be experimentally obtained according to the initial equilibrium position.

We have shown in previous studies, by using structural parameter identifiability concepts,[11,13,22] that the zeolitic layer thickness cannot be separated from the equilibrium parameters in the case of single component linear transient experiments.[1,2] Consequently, a specific transient experiment was proposed to estimate the zeolitic layer thickness based on the use of a very weakly adsorbed molecule like hydrogen.[1,2,20] Helium has also been used for the same purpose within the framework of the time lag technique.[23]

Finally, in order to perform the parameter estimation of the zeolitic layer, thermodynamic and transport parameters by time domain fitting,[22] we have developed and characterized a complete dynamic model of the equipment itself. The validity of this approach to characterize thermodynamic and diffusion properties within the Henry domain by using *n*-butane and isobutane as pure adsorbates, and the MFI composite membranes synthesized at IFP Energies nouvelles was, thus, tested.[1,2]

Let us notice that the question of mass-transfer modeling within the Wicke-Kallenbach set-up has been extensively addressed in the literature. As far as supported zeolite membranes are concerned, it has been shown that, in order to represent the highly nonlinear behavior of the diffusion process, Maxwell-Stefan approach has to be used.[24,25] It allows to take into account the influence of the loading on the diffusion process. The diffusion coefficients included in this description are considered as friction coefficients either between the diffusing species and the adsorbent or between the diffusing species. In some cases, it has been shown that the latter, that are often neglected, may have a significant influence on the diffusion process.[26,27] The confinement effect that can induce a strong loading influence on the Maxwell-Stefan approach (MS) diffusivities has also been studied by simulation.[28] A parametric study for binary mixtures has been provided in relation with transient experiments.[29] The slowing-down and speeding-up effect in binary mixtures have also been studied in the case of polar organic components diffusion through MFI composite tubular membranes.[30]

The possibility to determine experimentally the evolution of single components transport and thermodynamic properties of zeolite supported membranes with respect to the zeolitic layer loading by using our dynamic approach is checked. An extension of the method is also proposed in the case of binary mixtures. Normal butane and isobutane were chosen as test adsorbates.

This article is organized as follows. At first, a very brief description of the experimental set-up is provided since this description can be found elsewhere.[1,2] Second, the principle of the experiments that we perform in the linear domain for single components and mixtures is detailed. The linear mass-transfer model that is used for the parameter estimation is described. The structural analysis of the model with respect to the parameter estimation problem is also addressed. Finally, before concluding, the results and the proposed method are discussed.

## Principle of the Experiments

### *Experimental set-up*

The membrane module that is used for this study is represented in Figure 1. The zeolitic layers, made at IFP Energies nouvelles, were grown on the inner side of a tubular Pall Exekia T1-70 alumina asymmetric porous tube (length 150 mm, inner diameter 6.55 mm, and thickness 1.73 mm). The support tubing was enameled at both ends for sealing purposes. The zeolite crystals were synthesized inside the pores of the support according to the pore-plugging method.[3–5] The module was placed in the oven of a GC (HP 5890 Series II Gas Phase Chromatograph) in order to use the facilities of this apparatus (temperature regulation, detectors, and injection loop).

In the case of single component experiments, the thermal conductivity detector of the GC was used to perform the outlet concentration measurements after a calibration procedure.[1,2] In the case of binary mixtures, an infra red photometer (PIR 3502 from ABB) was used to measure the absorbance of the gas outlet mixture at, respectively, 970 $cm^{-1}$ and 1175 $cm^{-1}$ for *n*-butane and isobutane. The time constant of this apparatus is 20 ms so that it does not affect the time response of the measurements.

### *Linear experiments principle*

Let us first consider the single component experiments as illustrated in Figure 2. A gas carrier containing the component of interest feeds cocurrently both the inner and outer compartments. The zeolitic layer is in equilibrium with the gas according to what is ordinary designated as the baseline in inverse chromatography. This baseline is characterized by the composition of the gas carrier and corresponds to one point of the equilibrium curve. To this baseline, a concentration pulse at the retentate inlet is superimposed. This

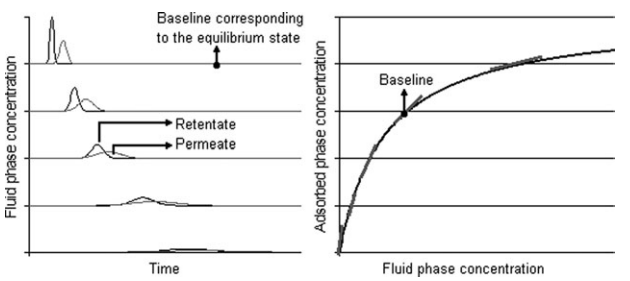


**Figure 2. Single component principle of the linear experiments according to the equilibrium baseline.**

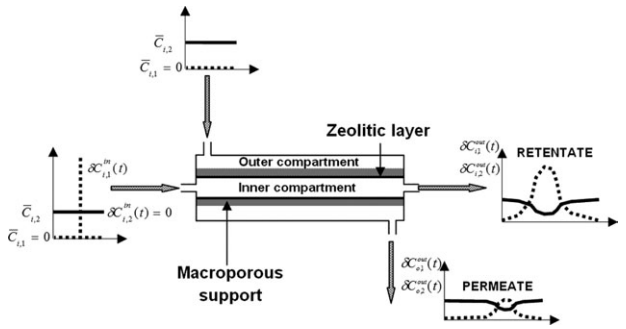


**Figure 3. Binary mixture pulse injection experiment principle (component 1: ▪▪▪▪▪▪, component 2: ——).**

concentration pulse is obtained by rapidly injecting a small amount of the adsorbate by using the GC injection loop. If the intensity of this pulse is sufficiently low, the response of the system will remain in the linear domain. The parameters that are extracted from this experiment are associated to the baseline point under consideration, and their evolution according to this point can be obtained experimentally. When the baseline point corresponds to an adsorbate-free membrane, that is, a pure gas carrier—the experiment is performed within the Henry domain.[1,2]

This technique can be easily extended to mixtures. The initial equilibrium point can be varied by choosing the composition of the gas carrier. The composition of the concentration pulse that is superimposed to this initial baseline can also be varied by adjusting the content of the injection loop. In order for the response to remain linear, the intensity of this pulse must also be low enough. In Figure 3, the technique is illustrated in the case of a binary mixture (components 1 and 2) by an example of configuration. The initial equilibrium is defined by the feed gas containing only component 2 and a low intensity concentration pulse containing component 1 only is superimposed at the retentate inlet. Both the concentrations of components 1 and 2 vary at the membrane module outlets after the initial equilibrium perturbation due to the component 1 injection.

## Dynamic model of the System

The characterization method that we propose is based on a time fitting of the parameters of a model to the dynamic experimental results. The experiments being performed within the linear domain, a model is first derived from first principles and is linearized in the vicinity of the initial equilibrium point. The model under consideration is made of two submodels: the model of the zeolitic layer and the model of the module. As far as the latter is described elsewhere,[1,2] we simply recall the main assumptions that are made. The estimation of the parameters of the module model from specific transient experiments is also described elsewhere.[1,2,20] We give more details about the zeolitic layer model to emphasize the way the parameters related to the zeolitic layer properties are estimated.

The model under consideration is isothermal since the membrane module is placed in the oven of a GC and maintained at a constant high temperature during the experiments. Furthermore, the inlet concentration pulses being of low intensity in order for the system to behave linearly, the temperature variations due to the adsorption–desorption phenomena can be neglected.

### *Dynamic model of the module*

The aim of this model is to take into account the influence of the inner and outer flows as well as that of the porous support on the dynamic response of the system. All the parameters included in this model are assumed to be constant and the resulting model is linear at the beginning.

*Retentate and permeate flows model.* In order to take into account the axial dispersion along the tube axial coordinate $z$, a serial arrangement of plug flows with axial dispersion has been used to represent the adsorbates' transport through the different sections of the inner and outer compartments. The axial dispersion coefficients of both the inner and outer compartments' flows have been previously experimentally determined. To this end, classical tracer experiments with hydrogen were performed by replacing the porous membrane by a stainless tube having the same dimensions.[1,2]

*Mass transfer within the porous support.* A lumped parameter model has been used to account for the accumulation of adsorbates within the macroporous support (see Figure 4 showing an equivalent electrical circuit of the macroporous support and the zeolitic layer model). Two mass-transfer coefficients have been introduced:

- $k_o$ is the mass-transfer coefficient between the outer compartment gas flow and the macroporous support;
- $k_s$ is the mass-transfer coefficient accounting for the diffusive gaseous transport through the macroporous support.

On the inner side of the membrane, equilibrium between the gas phase and the zeolitic layer is assumed. $k_o$ and $k_s$ have been estimated by performing low intensity pulse injections of hydrogen at the retentate inlet, the zeolitic layer being present. These experiments with hydrogen as tracer have also allowed estimating the zeolitic layer thickness.[1,2]

### *Dynamic model of the diffusion through the zeolitic layer*

The mathematical formulation of this model has to be well suited for the parameter estimation purpose, that is to say the model has to be structurally identifiable.[22] This property is not necessarily satisfied for first principles models. For example, we have shown that some classical chromatographic column models that are used for the single component inverse chromatography technique are not structurally

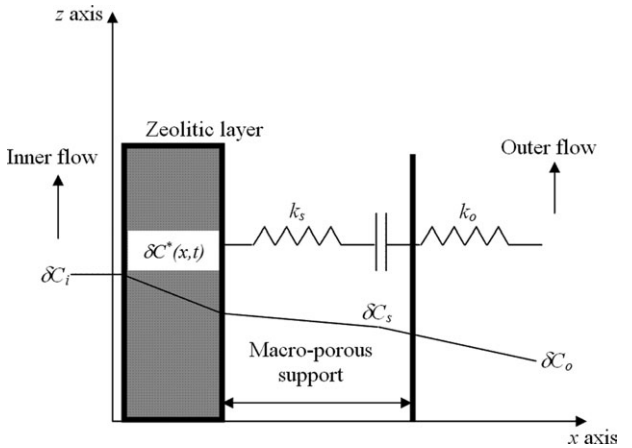


**Figure 4. Equivalent electrical circuit of the membrane dynamic model.**

identifable.[11,13] This lack of identifiability is due to the fact that the ordinary concentration variable $q_z$ is used as state variable to represent the adsorbent composition. In order to get a structurally identifiable model, the composition of the adsorbent has to be represented by $C^*$, the concentration of a fictitious gaseous phase that would be at equilibrium with the adsorbent phase at the same time and at the same spatial coordinate. This result has been extended to the supported membrane in the case of the single component linear model.[1,2] This change of state variable allows the composition discontinuity occurring at the gas–solid interface to be removed (see Figure 4) so that the model is as compact as possible with respect to the number of parameters. We want to emphasize on the fact that this change of state variable does not change the solution of the model equations. In particular, the simulated outlet concentrations' trajectories for a given set of known physical parameters are identical to the one given by the initial version of the model. It is said in the automatic control domain[22] that the input–output behavior of the two versions of the model is the same. On the contrary, due to the fact that only gaseous phases' inlet and outlet concentrations are measured, the version of the model based on the change of state variable that we propose is well suited for estimation purposes while the other one is overparametrized.

*Single component model* Let us consider the adsorbate material balance within the zeolitic layer

$$\begin{cases} \dfrac{\partial q_z}{\partial t} = -\nabla \cdot N_z \\ N_z = -\dfrac{D_z^{MS}(q_z) q_z}{RT} \cdot \nabla \mu_z = -\dfrac{D_z^{MS}(q_z) q_z}{RT} \cdot \dfrac{\partial \mu_z}{\partial q_z} \cdot \nabla q_z \end{cases} \quad (1)$$

The adsorbate flux $N_z$ is expressed according to the MS approach as a function of its chemical potential within the zeolitic layer $\mu_z$. The MS diffusivity itself can be a function of $q_z$.[24,25,31] The experiments are performed in the linear domain from a thermodynamic equilibrium initial condition characterized by the adsorbate constant concentration $\overline{q}_z$ and the corresponding gaseous phases constant concentration $\overline{C}_i = \overline{C}_o$. A linear version of Eq. 1 can be derived for $\delta q_z$, a small deviation of $q_z$ from $\overline{q}_z$ (see Figure 2)

$$\begin{cases} \frac{\partial q_z}{\partial t} = \frac{\partial (\delta q_z)}{\partial t} = -\nabla \cdot (\overline{N}_z + \delta N_z) = -\nabla \cdot (\delta N_z) \\ N_z = \delta N_z = -\frac{D_z^{MS}(\overline{q}_z + \delta q_z) \cdot (\overline{q}_z + \delta q_z)}{RT} \cdot \nabla (\overline{\mu}_z + \delta \mu_z) \\ \approx -\frac{D_z^{MS}(\overline{q}_z) \cdot \overline{q}_z}{RT} \cdot \frac{\partial \mu_z}{\partial q} \Big|_{q_z = \overline{q}_z} \cdot \nabla (\delta q_z) \end{cases} \quad (2)$$

As a matter of fact, as the initial steady state is also an equilibrium state, we have

$$\begin{cases} \overline{N}_z = 0 \\ \nabla (\overline{\mu}_z) = 0 \end{cases} \quad (3)$$

By denoting $D_z \Big|_{q_z = \overline{q_z}} = \frac{D_z^{MS}(\overline{q_z}) \cdot \overline{q_z}}{RT} \cdot \frac{\partial \mu_z}{\partial q_z} \Big|_{q_z = \overline{q_z}}$, the diffusion coefficient within the zeolitic layer of the linear model or Fick diffusion coefficient, we obtain for the linear model

$$\begin{cases} \dfrac{\partial (\delta q_z)}{\partial t} = -\nabla \cdot (\delta N_z) \\ \delta N_z \approx -D_z \big|_{q_z = \overline{q}_z} \cdot \nabla (\delta q_z) \end{cases} \quad (4)$$

In order to preserve the structural identifiability properties of the linearized model, we define the following change of state variable[1,2,11,13]

$$\delta q_z = \frac{\partial q_z}{\partial C^*} \Big|_{C^* = \overline{C}^*} \cdot \delta C^* = \kappa \big|_{C^* = \overline{C}^*} \cdot \delta C^* \quad (5)$$

where $C^*$ is the concentration of a fictitious gas that would be in equilibrium with the zeolitic layer at the concentration $q_z$. Equation 5 is the equilibrium relation between the small deviations $\delta q_z$ and $\delta C^*$. As a matter of fact, if one considers the thermodynamic equilibrium relation $q_z = q_z(C^*)$, its linearized version is straightforward (see Figure 2)

$$q_z(C^*) = \overline{q}_z(\overline{C}^*) + \delta q_z \approx \overline{q}_z(\overline{C}^*) + \frac{\partial q_z}{\partial C^*} \Big|_{C^* = \overline{C}^*} \cdot \delta C^* \quad (6)$$

Finally, the linear dynamic model of the zeolitic layer expressed with respect to $\delta C^*$ is as follows where the initial equilibrium condition is now represented by $\overline{C}^*$ instead of $\overline{q}_z$

$$\frac{\partial (\delta C^*)}{\partial t} = D_z \big|_{C^* = \overline{C}^*} \cdot \Delta (\delta C^*) \quad (7)$$

A simple one-dimensional model in Cartesian coordinates has turned to be sufficient for the zeolitic layer so that a dimensionless version of Eq. 7 can be expressed as follows

$$\frac{\partial (\delta C^*)}{\partial t} = \frac{D_z \big|_{C^* = \overline{C}^*}}{e_z^2} \cdot \frac{\partial^2 (\delta C^*)}{\partial \eta^2} = \frac{1}{\tau_z \big|_{C^* = \overline{C}^*}} \cdot \frac{\partial^2 (\delta C^*)}{\partial \eta^2} \quad (8)$$

with $\eta = \frac{x}{e_z}, 0 \le x \le e_z$..

The dimensionless boundary conditions are as follows

$$\begin{cases} \delta C_i(t,z) = \delta C^*(t, \eta = 0) \\ k_s \cdot \varepsilon \cdot (\delta C_s(t,z) - \delta C^*(t, \eta = 1)) = \frac{D_z \big|_{C^* = \overline{C}^*} \cdot \kappa \big|_{C^* = \overline{C}^*}}{e_z} \cdot \frac{\partial (\delta C^*)}{\partial \eta} = B_z \big|_{C^* = \overline{C}^*} \cdot \frac{\partial (\delta C^*)}{\partial \eta} \end{cases} \quad (9)$$

where $\delta C_s(t,z)$ and $\delta C_i(t,z)$ are, respectively, the small deviations of the macroporous tube and inner compartment concentrations at the $z$ axial position of the membrane.

*Binary mixture model.* Since the initial steady state corresponds to an equilibrium point, Eqs. 3 hold for the two components of the mixture so that the balance equations can be written according to the small deviations

$$\frac{\partial (\delta q_{z,j})}{\partial t} = -\nabla \cdot (\delta N_{z,j}) \quad j = 1,2 \quad (10)$$

We assume that the above-proposed change of state variables is also valid for mixtures in order for the identifiability properties of the model to be preserved. As far as small deviations are concerned, we define the following change of the zeolitic layer composition state variables

$$\begin{pmatrix} \delta C_1^* \\ \delta C_2^* \end{pmatrix} = \overline{\gamma} \cdot \begin{pmatrix} \delta q_{z,1} \\ \delta q_{z,2} \end{pmatrix} \quad (11)$$

where $\overline{\gamma} = \begin{pmatrix} \frac{\partial C_1^*}{\partial q_{z,1}}\Big|_{C_1^*=\overline{C}_1^*,C_2^*=\overline{C}_2^*} & \frac{\partial C_1^*}{\partial q_{z,2}}\Big|_{C_1^*=\overline{C}_1^*,C_2^*=\overline{C}_2^*} \\ \frac{\partial C_2^*}{\partial q_{z,1}}\Big|_{C_1^*=\overline{C}_1^*,C_2^*=\overline{C}_2^*} & \frac{\partial C_2^*}{\partial q_{z,2}}\Big|_{C_1^*=\overline{C}_1^*,C_2^*=\overline{C}_2^*} \end{pmatrix}$ is a constant matrix evaluated at the initial equilibrium point represented by the fictitious gaseous phase concentrations $\overline{C}_1^*$ and $\overline{C}_2^*$.

Let us now consider the expression of the flux $N_{z,j}$ as it is given by the MS approach.[24] If $u_{z,j}$ is the velocity of component $j$ within the zeolitic layer, the following steady-state momentum balances for the two components are as follows

$$\begin{cases} \dfrac{-\nabla\mu_{z,1}}{RT} = \dfrac{\theta_2\cdot(u_{z,1}-u_{z,2})}{D_{12}} + \dfrac{u_{z,1}\cdot(1-\theta_1-\theta_2)}{D_1} = u_{z,1}\cdot\left(\dfrac{\theta_2}{D_{12}} + \dfrac{(1-\theta_1-\theta_2)}{D_1}\right) - u_{z,2}\cdot\left(\dfrac{\theta_2}{D_{12}}\right) \\ \dfrac{-\nabla\mu_{z,2}}{RT} = \dfrac{\theta_1\cdot(u_{z,2}-u_{z,1})}{D_2} + \dfrac{u_{z,2}\cdot(1-\theta_1-\theta_2)}{D_2} = u_{z,1}\cdot\left(\dfrac{\theta_1}{D_{21}}\right) + u_{z,2}\cdot\left(\dfrac{\theta_1}{D_{12}} + \dfrac{(1-\theta_1-\theta_2)}{D_2}\right) \\ N_{z,j} = q_{z,j}\cdot u_{z,j} \end{cases} \tag{12}$$

where $\theta_j = \frac{q_{z,j}}{q_j^{sat}}$ is the loading of the $j$ component with respect to a maximum loading that can possibly depend on the adsorbate.[27] In this formulation, the friction force due to the adsorbent is assumed to be proportional to the vacant sites' fraction.[32] These equations can be inverted in order to express the flux as a function of $\bigtriangledown\mu_{z,1}$ and $\bigtriangledown\mu_{z,2}$

$$\begin{pmatrix} N_{z,1} \\ N_{z,2} \end{pmatrix} = -\begin{pmatrix} \beta_{11} & \beta_{12} \\ \beta_{21} & \beta_{22} \end{pmatrix}\begin{pmatrix} \frac{\nabla\mu_{z,1}}{RT} \\ \frac{\nabla\mu_{z,2}}{RT} \end{pmatrix} \tag{13}$$

In order to use the change of state variable that we propose, the chemical potential gradient is simply expressed as $\frac{\nabla\mu_{z,j}}{RT} = \frac{\nabla C_j^*}{C_j^*}$ as the fictitious gaseous phase at concentrations $C_j^*$ is assumed to be ideal. Then, Eq. 13 becomes

$$\begin{pmatrix} N_{z,1} \\ N_{z,2} \end{pmatrix} = -\begin{pmatrix} \beta_{11} & \beta_{12} \\ \beta_{21} & \beta_{22} \end{pmatrix}\begin{pmatrix} \frac{\nabla C_1^*}{C_1^*} \\ \frac{\nabla C_2^*}{C_2^*} \end{pmatrix} = -\begin{pmatrix} \frac{\beta_{11}}{C_1^*} & \frac{\beta_{12}}{C_2^*} \\ \frac{\beta_{21}}{C_1^*} & \frac{\beta_{22}}{C_2^*} \end{pmatrix}\begin{pmatrix} \nabla C_1^* \\ \nabla C_2^* \end{pmatrix} \tag{14}$$

Finally, the small deviations of the fluxes with respect to the initial equilibrium are given by

$$\begin{pmatrix} \delta N_{z,1} \\ \delta N_{z,2} \end{pmatrix} = -\begin{pmatrix} \frac{\overline{\beta}_{11}}{\overline{C}_1^*} & \frac{\overline{\beta}_{12}}{\overline{C}_2^*} \\ \frac{\overline{\beta}_{21}}{\overline{C}_1^*} & \frac{\overline{\beta}_{22}}{\overline{C}_2^*} \end{pmatrix}\begin{pmatrix} \nabla(\delta C_1^*) \\ \nabla(\delta C_2^*) \end{pmatrix} \tag{15}$$

By combining Eqs. 10, 11, and 15, one find the binary mixture planar linearized one-dimensional mass-transfer model of the zeolitic layer as expressed with respect to $\delta C_1^*$ and $\delta C_2^*$

$$\begin{pmatrix} \frac{\partial(\delta C_1^*)}{\partial t} \\ \frac{\partial(\delta C_2^*)}{\partial t} \end{pmatrix} = \begin{pmatrix} \overline{\gamma}_{11} & \overline{\gamma}_{12} \\ \overline{\gamma}_{21} & \overline{\gamma}_{22} \end{pmatrix}\begin{pmatrix} \frac{\overline{\beta}_{11}}{\overline{C}_1^*} & \frac{\overline{\beta}_{12}}{\overline{C}_2^*} \\ \frac{\overline{\beta}_{21}}{\overline{C}_1^*} & \frac{\overline{\beta}_{22}}{\overline{C}_2^*} \end{pmatrix}\begin{pmatrix} \frac{\partial^2(\delta C_1^*)}{\partial x^2} \\ \frac{\partial^2(\delta C_1^*)}{\partial x^2} \end{pmatrix} \tag{16}$$

The dimensionless form of Eqs. 16 is then as follows

$$\begin{pmatrix} \frac{\partial(\delta C_1^*)}{\partial t} \\ \frac{\partial(\delta C_2^*)}{\partial t} \end{pmatrix} = \begin{pmatrix} \frac{1}{\overline{\tau}_{z,11}} & \frac{1}{\overline{\tau}_{z,12}} \\ \frac{1}{\overline{\tau}_{z,21}} & \frac{1}{\overline{\tau}_{z,2}} \end{pmatrix}\begin{pmatrix} \frac{\partial^2(\delta C_1^*)}{\partial \eta^2} \\ \frac{\partial^2(\delta C_1^*)}{\partial \eta^2} \end{pmatrix} \tag{17}$$

where $\begin{pmatrix} \frac{1}{\overline{\tau}_{z,11}} & \frac{1}{\overline{\tau}_{z,12}} \\ \frac{1}{\overline{\tau}_{z,21}} & \frac{1}{\overline{\tau}_{z,2}} \end{pmatrix} = \begin{pmatrix} \overline{\gamma}_{11} & \overline{\gamma}_{12} \\ \overline{\gamma}_{21} & \overline{\gamma}_{22} \end{pmatrix}\begin{pmatrix} \frac{\overline{\beta}_{11}}{\overline{C}_1^* e_z^2} & \frac{\overline{\beta}_{12}}{\overline{C}_2^* e_z^2} \\ \frac{\overline{\beta}_{21}}{\overline{C}_1^* e_z^2} & \frac{\overline{\beta}_{22}}{\overline{C}_2^* e_z^2} \end{pmatrix}$ is a constant matrix containing the inverse of four diffusion time constants. The corresponding dimensionless boundary conditions are as follows

$$\begin{cases} \begin{pmatrix} \frac{\overline{\beta}_{11}}{\overline{C}_1^* e_z} & \frac{\overline{\beta}_{12}}{\overline{C}_2^* e_z} \\ \frac{\overline{\beta}_{21}}{\overline{C}_1^* e_z} & \frac{\overline{\beta}_{22}}{\overline{C}_2^* e_z} \end{pmatrix}\begin{pmatrix} \frac{\partial(\delta C_1^*)}{\partial \eta}(\eta=1,t) \\ \frac{\partial(\delta C_2^*)}{\partial \eta}(\eta=1,t) \end{pmatrix} = \begin{pmatrix} \varepsilon\cdot k_{s1}\cdot(\delta C_{s,1}(z,t) - \delta C_1^*(\eta=1,t)) \\ \varepsilon\cdot k_{s2}\cdot(\delta C_{s,2}(z,t) - \delta C_2^*(\eta=1,t)) \end{pmatrix} \\ \delta C_{i,1}(t,z) = \delta C_1^*(t,\eta=0) \\ \delta C_{i,2}(t,z) = \delta C_2^*(t,\eta=0) \end{cases} \tag{18}$$

Let us now consider the way the parameter estimation is performed.

## Estimation Procedure

### *Numerical solution of the model equations*

The parameters that are estimated are those of the linearized models described above from the linear domain experiments by applying a time domain fitting. The set of partial differential equations of the models are first reduced to a set of algebraic equations by applying an implicit finite difference scheme. The parameter estimation is performed by using the Levenberg-Marquardt algorithm. The code is written with the Fortran® language and the IMSL® library (International Mathematical Subroutine Library) BCLSF algorithm is used for the optimization. This algorithm solves a

nonlinear least squares problem subject to bounds on the variables using a modified Levenberg-Marquardt algorithm and a finite-difference Jacobian.

### *Single component experiments*

The advantage of the proposed change of state variable for the zeolitic layer appears if one considers the initial conditions of the transient experiments. As these conditions correspond to an equilibrium point of the zeolitic layer with the gaseous phases, we have $\overline{C}_i = \overline{C}_o = \overline{C}^*(t = 0,\eta)$. The initial values of all the state variables are measured, which is a great advantage for the estimation procedure, as these initial conditions that have to be used as initial conditions for the simulation does not depend on the parameters to be estimated.

The zeolitic layer properties are represented by the two macro-parameters $\tau_z = \frac{e_z^2}{D_z}$ and $B_z = \frac{D_z \cdot \kappa}{e_z}$ (see Eqs. 8 and 9). We want to emphasize at this point, that neither a thermodynamic model nor a model for $D_z^{MS}$ have been postulated for deriving the linearized model. A time domain fitting of the two macro-parameters $\tau_z$ and $B_z$ is first performed. $D_z$ and $\kappa$ are then deduced as the other parameters of the model (particularly the zeolitic layer thickness $e_z$) have been estimated from previous independent dynamic experiments.[1,2] Then, the evolution of $\tau_z$ and $B_z$ with $\overline{C}^*$ can be observed. This way of determining physico-chemical parameters (or micro-parameters) from the estimates of dimensional or dimensionless groups (macro-parameters) has proved to be more efficient.[11,13,22]

### *Binary mixture experiments*

The advantage of the change of state variables that we propose as pointed out in the case of single component experiments is also available with respect to the initial condition measurements for the binary mixture experiments.

The zeolitic layer properties are entirely contained in the two matrices $\boldsymbol{\tau}^{-1} = \begin{pmatrix} \frac{1}{\overline{\tau}_{z,11}} & \frac{1}{\overline{\tau}_{z,12}} \\ \frac{1}{\overline{\tau}_{z,21}} & \frac{1}{\overline{\tau}_{z,2}} \end{pmatrix}$ and $\boldsymbol{B} = \begin{pmatrix} \frac{\overline{\beta}_{11}}{\overline{C}_1^* e_z} & \frac{\overline{\beta}_{12}}{\overline{C}_2^* e_z} \\ \frac{\overline{\beta}_{21}}{\overline{C}_1^* e_z} & \frac{\overline{\beta}_{22}}{\overline{C}_2^* e_z} \end{pmatrix}$. As eight parameters have to be estimated, a blind estimation procedure as the one we can apply in the case of the single component experiments does not seem to be reliable so that a preliminary analysis has to be performed. For example, by assuming the binary Langmuir model with different saturation loadings for the two components,[27] one can derive the corresponding expressions of the matrixes $\boldsymbol{\tau}^{-1}$ and $\boldsymbol{B}$ (see Appendix).

One has to notice that only the $\boldsymbol{B}$ matrix depends on the saturation loadings $q_1^{sat}$ and $q_2^{sat}$. From these expressions, one can perform the analysis of some specific situations. If the transient experiments are performed within the Henry domain, that is, $\overline{C}_1^* = \overline{C}_2^* = 0$, the parameter matrices are as follows

$$\boldsymbol{B} = \begin{pmatrix} \frac{q_1^{sat} b_1 D_1}{e_z} & 0 \\ 0 & \frac{q_2^{sat} b_2 D_2}{e_z} \end{pmatrix} \tag{19}$$

$$\boldsymbol{\tau}^{-1} = \begin{pmatrix} \frac{D_1}{e_z^2} & 0 \\ 0 & \frac{D_2}{e_z^2} \end{pmatrix} \tag{20}$$

The two components are transported independently according to the Fick's law associated to a linear equilibrium equation. The total number of parameters is then reduced to 4. The diffusion coefficient $D_{12}$ is in particular eliminated. $D_1$ and $D_2$ can be calculated from the estimated values of $\frac{1}{\overline{\tau}_{z,11}}$ and $\frac{1}{\overline{\tau}_{z,22}}$ but it is impossible to separate $q_j^{sat}$ and $b_j$.

If the membrane content is far from the saturation loading, the influence of the momentum exchange between the adsorbates as represented by the exchange coefficient $D_{12}$ can be neglected.[33] In this case, for any initial equilibrium conditions, the two matrices of parameters become

$$\boldsymbol{B} = \begin{pmatrix} \frac{q_1^{sat} b_1 D_1}{e_z} & 0 \\ 0 & \frac{q_2^{sat} b_2 D_2}{e_z} \end{pmatrix} \tag{21}$$

$$\boldsymbol{\tau}^{-1} = \begin{pmatrix} \frac{D_1(1+b_1\overline{C}_1^*+b_2\overline{C}_2^*)(1+b_1\overline{C}_1^*)}{e_z^2} & \frac{D_2(1+b_1\overline{C}_1^*+b_2\overline{C}_2^*)b_2\overline{C}_1^*}{e_z^2} \\ \frac{D_1(1+b_1\overline{C}_1^*+b_2\overline{C}_2^*)b_1\overline{C}_2^*}{e_z^2} & \frac{D_2(1+b_1\overline{C}_1^*+b_2\overline{C}_2^*)(1+b_2\overline{C}_2^*)}{e_z^2} \end{pmatrix} \tag{22}$$

An interesting property is that the $\boldsymbol{\tau}^{-1}$ matrix remains full while the $\boldsymbol{B}$ matrix becomes diagonal and does not depend anymore on the initial equilibrium conditions.

If $\overline{C}_2^* = 0$, that is to say the initial equilibrium situation is such that the system does not contain the component 2, the parameter matrices become

$$\boldsymbol{B} = \begin{pmatrix} \frac{q_1^{sat} b_1 \left(\frac{b_1\overline{C}_1^*}{D_{21}} + \frac{1}{D_2}\right)}{e_z \left(\frac{b_1\overline{C}_1^*}{D_1 D_{21}} + \frac{1}{D_1 D_2}\right)} & \frac{q_1^{sat} b_1 b_2 \overline{C}_1^*}{e_z D_{12} \left(\frac{b_1\overline{C}_1^*}{D_1 D_{21}} + \frac{1}{D_1 D_2}\right)} \\ 0 & \frac{\frac{q_2^{sat} b_2}{D_1}}{e_z \left(\frac{b_1\overline{C}_1^*}{D_1 D_{21}} + \frac{1}{D_1 D_2}\right)} \end{pmatrix} \tag{23}$$

$$\boldsymbol{\tau}^{-1} = \begin{pmatrix} \frac{(1+b_1\overline{C}_1^*)}{e_z^2 \left(\frac{b_1\overline{C}_1^*}{D_1 D_{21}} + \frac{1}{D_1 D_2}\right)} \left((1 + b_1\overline{C}_1^*)\left(\frac{b_1\overline{C}_1^*}{D_{21}} + \frac{1}{D_2}\right)\right) & \frac{(1+b_1\overline{C}_1^*)b_2\overline{C}_1^*}{e_z^2 \left(\frac{b_1\overline{C}_1^*}{D_1 D_{21}} + \frac{1}{D_1 D_2}\right)} \left(\frac{(1+b_1\overline{C}_1^*)}{D_{12}} + \frac{1}{D_1}\right) \\ 0 & \frac{(1+b_1\overline{C}_1^*)}{e_z^2 D_1 \left(\frac{b_1\overline{C}_1^*}{D_1 D_{21}} + \frac{1}{D_1 D_2}\right)} \end{pmatrix} \tag{24}$$

Two parameters are eliminated in this case. Similarly, if $\overline{C}_1^* = 0$, two parameters are also eliminated.

## Results

Two membranes have been used to test the proposed approach, respectively, denoted M1 and M2. Their properties can differ as they have been synthesized under different conditions (M1: 1 $SiO_2$/0.4 tetrapropylammonium hydroxide (TPAOH)/18.3 $H_2O$, M2: 1 $SiO_2$/0.4 TPAOH/63.7 $H_2O$). For example, their effective thickness have been found to be different (respectively $e_z^{M1} = 26$ $\mu$m and $e_z^{M2} = 9.8$ $\mu$m for membranes M1 and M2) by performing transient experiments with

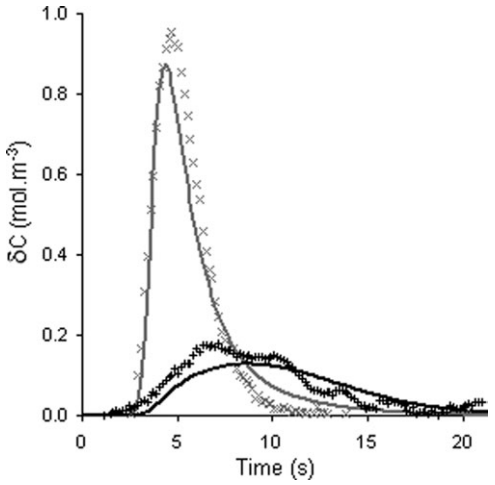


**Figure 5. Outlet *n*-butane concentration variations (membrane M1, $T$ = 200°C, $P$ = 1 atm, $\overline{C}_i = \overline{C}_o$ = 5.15 mol m$^{-3}$, continuous lines: simulation, ×: retentate experimental values, +: permeate experimental values).**

hydrogen as a weakly adsorbed tracer.[1,2,20] The experiments that are shown here have been carried out at atmospheric pressure and for a temperature of 200°C.

### *Single* n-*butane experiments*

*Linear model parameters estimation.* One can see in Figure 5 an example of transient behavior of the M1 composite membrane outlet concentrations in the case of *n*-butane when a concentration pulse is superimposed to the baseline at $t = 0$ at the retentate inlet. This baseline is characterized by the retentate and permeate initial equilibrium concentrations $\overline{C}_i = \overline{C}_o = \overline{C}^* = 5.15$ mol m$^{-3}$. The experimental outlet concentrations are close to those given by the model after the unknown parameters $\tau_z$ and $B_z$ have been estimated. Such transient experiments have been performed for different initial conditions in order to get the experimental evolution of $\kappa$ and $D_z$ with respect to the baseline concentration. This baseline concentration is directly related to the membrane equilibrium loading $\overline{q}_z$.

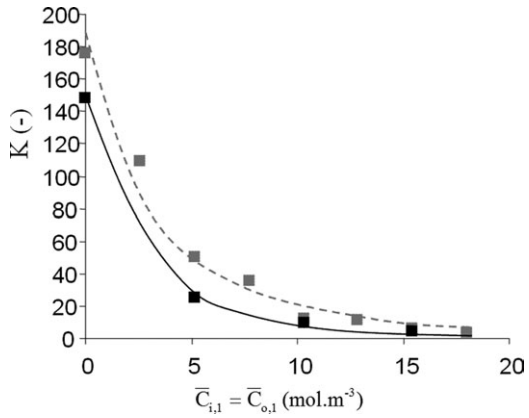


**Figure 6. Experimental *n*-butane equilibrium curve slopes according to the equilibrium gas phase concentration $\overline{C}_{i,1} = \overline{C}_{o,1}$ ($T$ = 200°C, $P$ = 1 atm. M1 membrane, ■: experimental values, —: monosite Langmuir model. M2 membrane, ■: experimental values, — -: monosite Langmuir model).**

**Table 1. M1 and M2 Membranes Pure *n*-Butane Monosite Langmuir Model Estimated Parameters**

| Membrane M1 | | Membrane M2 | |
|---|---|---|---|
| $q_{sat}$ | $b$ (m$^3$ mol$^{-1}$) | $q_{sat}$ | $b$ (m$^3$ mol$^{-1}$) |
| 600 mol m$^{-3}$ (0.33 mol kg$^{-1}$) | 0.25 | 900 mol m$^{-3}$ (0.5 mol kg$^{-1}$) | 0.21 |

*Parameters a posteriori analysis.* The variation of $\kappa$ according to $\overline{C}^* = \overline{C}_i = \overline{C}_o$ is shown in Figure 6 for the two membranes M1 and M2. As $\kappa$ is the first derivative of the adsorbate equilibrium concentration with respect to the gaseous phase concentration, the experimental results for $\kappa$ are compatible with a type-I equilibrium behavior.[34–37] Within the concentration interval that we have studied, such behavior can, for example, be correctly represented by the monosite Langmuir model (see Figure 6) by using the parameters that are given in Table 1 and according to the following relations

$$\overline{q}_z = q^{sat}\frac{b\overline{C}^*}{1+b\overline{C}^*} \qquad \kappa(\overline{C}^*) = q^{sat}\frac{b}{(1+b\overline{C}^*)^2} \tag{25}$$

We cannot extrapolate our results beyond this interval and consider a possible multisite situation. The $b$ parameter that is obtained is roughly the same for the two membranes while the saturation concentration is different. As the two membranes have been synthesized according to different conditions, they can exhibit different adsorptive properties. Nevertheless, the values that we obtain for $q^{sat}$ are lower than those obtained at 200°C for *n*-butane adsorption on silicalite-1[34] (0.87 mol kg$^{-1}$) or in the case of self-supporting MFI membranes (1.0 mol kg$^{-1}$).[35] The influence of the support itself on the properties of the zeolitic layer has been observed as it can lead to a variation of the zeolite Si/Al ratio due to the introduction of Al atoms in the zeolitic layer from the support itself.[38] Depending on the synthesis conditions as well as the precursor gel composition, the mean Si/Al ratio of the membranes can vary between 11 and 1000.[39–41] Such variation of the Si/Al ratio is known to have a great influence on the transport properties of the membranes.[38–40,42] Another explanation is the fact that our experiments have been performed for a *n*-butane, whose gaseous phase partial pressure is lower then 80 kPa. If one considers the already mentioned data for *n*-butane adsorption in silicalite-1 at 200°C,[34] it can be seen that the saturation is not reached even at 200 kPa so that the estimation of $q^{sat}$ can be affected by this high pressure extrapolation.

The order of magnitude of $b$ is the same as available data published previously in the literature.[6] Let us notice that the Si/Al ratio can also have a great influence on the zero loading slope of the equilibrium curve. For example, the saturation is reached for a rather lower value of pressure (about 40 kPa) in the case of self-supporting MFI membranes[35] while it is reached after 200 kPa in silicalite-1 at 200°C.[34]

In Figure 7, the variation of the Fickian diffusion coefficient of the *n*-butane through the zeolitic layers of the M1 and M2 membranes is shown. It can be seen that $D_z$ increases with the *n*-butane initial equilibrium concentration in the gaseous phase. This behavior is also in accordance with previous literature results.[43] A similar behavior has also been experimentally obtained for diffusion of branched

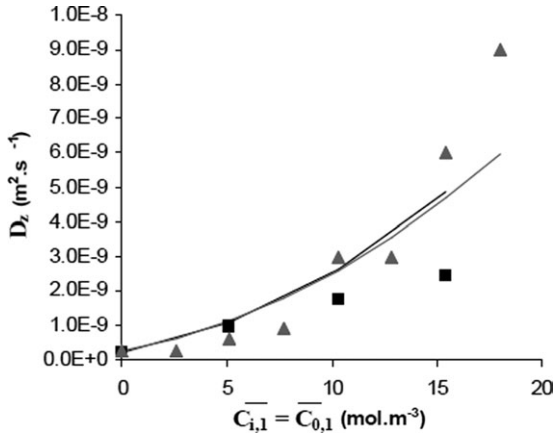


**Figure 7. Experimental *n*-butane Fick diffusion coefficient variation according to the equilibrium gas phase concentration $\overline{C}_{i,1} = \overline{C}_{o,1}$ ($T$ = 200°C, $P$ = 1 atm. M1 membrane, experimental values: ■, M2 membrane, experimental values: ▲. Continuous lines: Fick diffusion coefficient variation according to $\frac{1}{(1-\theta)^2}$ for the two membranes).**

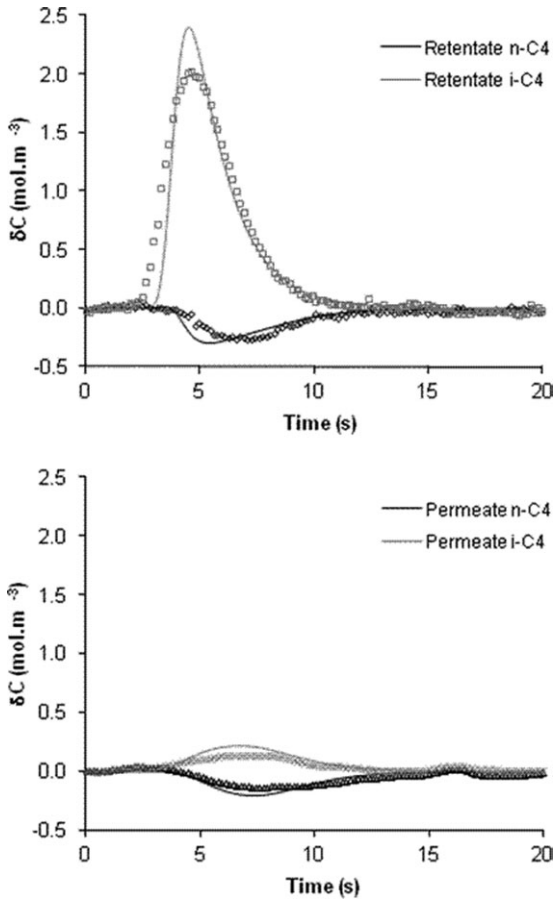


**Figure 8. *n*-Butane and isobutane outlet concentrations variations (M2 membrane, $T$ = 200°C, $P$ = 1 atm, $\overline{C}_{i,1} = \overline{C}_{o,1}$ = 5.15 mol $m^{-3}$, $\overline{C}_{i,2} = \overline{C}_{o,2}$ = 0, pure isobutane pulse injection, continuous lines: simulation, points: experimental results).**

**Table 2. M2 Membrane Model Estimated Parameters for the Binary Case**

| Parameter | Estimated value |
|---|---|
| $B_{z,1}$ (m $s^{-1}$) | $1.5 \times 10^{-3}$ |
| $B_{z,2}$ (m $s^{-1}$) | $5.1 \times 10^{-4}$ |
| $\tau_{z,11}$ (s) | $2.7 \times 10^{-2}$ |
| $\tau_{z,12}$ (s) | 9.6 |
| $\tau_{z,21}$ (s) | 459.6 |
| $\tau_{z,22}$ (s) | 4.8 |

paraffins in silicalite-1 by using the inverse chromatographic technique in the linear domain.[12] On the one hand, by considering the Langmuir monosite model, on the other hand, by assuming that the MS friction coefficient is proportional to the vacant site loading according to $D_z^{MS}(\theta) = \frac{D_z^{MS}(0)}{(1-\theta)}$,[32] the Fick diffusion coefficient should be a function of $\frac{1}{(1-\theta)^2}$. One can see in Figure 7 that this behavior seems to be experimentally confirmed. As far as the Fick diffusion coefficient variation amplitude is concerned, one can consider that the two membranes M1 and M2 behave similarly.

### n-*Butane/isobutane mixtures*

*Linear model parameters estimation.* The binary mixture experiments have been carried out by using the M2 membrane. One can see in Figure 8 an example of binary dynamic experiment. The baseline is made of a gas carrier only transporting *n*-butane at a concentration of $\overline{C}_{i,1} = \overline{C}_{o,1} = 5.15$ mol $m^{-3}$ so that the zeolitic layer initially contains only *n*-butane. A short pulse of pure isobutane is then superimposed at the inlet of the retentate flow. Both the *n*-butane and isobutane are transported toward the module outlet as it can be seen in Figure 8 as the initial equilibrium is perturbed by the isobutane injection. The isobutane quantity that is injected is very low while the initial equilibrium concentration of *n*-butane in the gas phase corresponds to a rather low partial pressure of 20,252 Pa. Consequently, we have assumed that in these conditions, the zeolitic layer loading was far from saturation conditions so that the influence of the exchange coefficient $D_{12}$ can be neglected.[33] In this case, the matrices to be estimated are given by Eqs. 21 and 22 within the framework of the preliminary analysis that we have proposed. We have performed the estimation of the two diagonal terms of the $\boldsymbol{B}$ matrix and of the four terms of the $\tau^{-1}$ matrix. The obtained time domain fitting is considered to be satisfactory (see Figure 8), and the corresponding estimated values of the parameters being given in Table 2. In order to compare our model with other experimental data that we have obtained, the estimation results given in Table 2 have been used to extract the parameters of the binary Langmuir model. Within the framework of this model, the two matrices $\tau^{-1}$ and $\boldsymbol{B}$ can be expressed as follows in the conditions of the experiments represented on Figure 8, that is, $\overline{C}_2^* = 0$:

$$\tau^{-1} = \begin{pmatrix} \frac{D_1 \cdot (1+b_1\overline{C}_1^*)^2}{e_z^2} & \frac{D_2 b_2 \overline{C}_1^* \cdot (1+b_1\overline{C}_1^*)}{e_z^2} \\ 0 & \frac{D_2 \cdot (1+b_1\overline{C}_1^*)}{e_z^2} \end{pmatrix} \tag{26}$$

$$\boldsymbol{B} = \begin{pmatrix} \frac{q_1^{sat} b_1 D_1}{e_z} & 0 \\ 0 & \frac{q_2^{sat} b_2 D_2}{e_z} \end{pmatrix} \tag{27}$$

It can be seen that the parameters $\overline{B}_{z,1} = \frac{q_1^{sat} b_1 D_1}{e_z}$ and $\overline{B}_{z,2} = \frac{q_2^{sat} b_2 D_2}{e_z}$ involved in the boundary conditions are not supposed to

depend on the initial conditions. Consequently, their estimated values from the experiment represented in Figure 8 can be directly used for the simulations of the other experiments. The theoretical value of $\overline{\tau}_{z,21}$ within the binary Langmuir model is infinite so that $\frac{1}{\overline{\tau}_{z,21}} \rightarrow 0$. This result is well correlated with the estimated value of $\overline{\tau}_{z,21}$ that is rather high when compared to the other times constants (see Table 2). Since the theoretical ratio $\frac{\frac{1}{\overline{\tau}_{z,12}}}{\frac{1}{\overline{\tau}_{z,22}}} = b_2\overline{C}_1^*$, one can calculate $b_2 = 9.7 \times 10^{-2}$ m$^3$ mol$^{-1}$ from the estimated values of $\overline{\tau}_{z,12}$ and $\overline{\tau}_{z,22}$, since $\overline{C}_1^*$ is measured. They are several ways to calculate $b_1$ from the estimated values of the diffusion time constants. They all require the values of the zero loading diffusion coefficients $D_1$ or $D_2$ (see Eq. 26). We have assumed that the zero loading diffusion coefficient obtained for the pure *n*-butane experiments in the case of the M2 membrane, that is, $D_1 = 2.6 \times 10^{-10}$ m$^2$ s$^{-1}$ (see Figure 7), can be used for the zero loading coefficient for the binary mixture. Considering the estimated value of $\overline{\tau}_{z,11}$ that is theoretically equal to $\frac{e_z^2}{D_1 \cdot (1+b_1\overline{C}_1^*)^2}$ within the framework of the binary Langmuir model, we have obtained a rather consistent value for $b_1$, that is, $b_1 = 0.52$ m$^3$ mol$^{-1}$. Finally, by considering the estimated value of $\overline{\tau}_{z,22}$ that is theoretically equal to $\frac{e_z^2}{D_2 \cdot (1+b_1\overline{C}_1^*)}$, one can get the estimate of the isobutane zero loading diffusion coefficient $D_2 = 5.4 \times 10^{-12}$ m$^2$ s$^{-1}$. In the literature, $D_2$ has been found between $5 \times 10^{-12}$ and $5 \times 10^{-11}$ m$^2$ s$^{-1}$ from single component experiments (see Figure 17 in our previous paper[1]). The value that we have obtained from binary experiments is then consistent with these results.

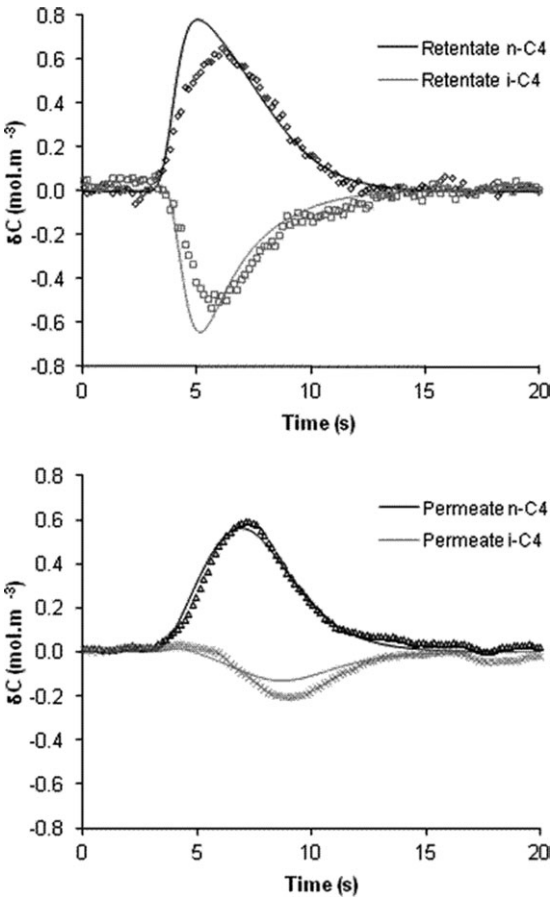


**Figure 9. *n*-Butane and isobutane outlet concentrations variations (M2 membrane, $T$ = 200°C, $P$ = 1 atm, $\overline{C}_{i,1} = \overline{C}_{o,1} = 0$, $\overline{C}_{i,2} = \overline{C}_{o,2} = 5.15$ mol m$^{-3}$, pure *n*-butane pulse injection, continuous lines: simulation, points: experimental results).**

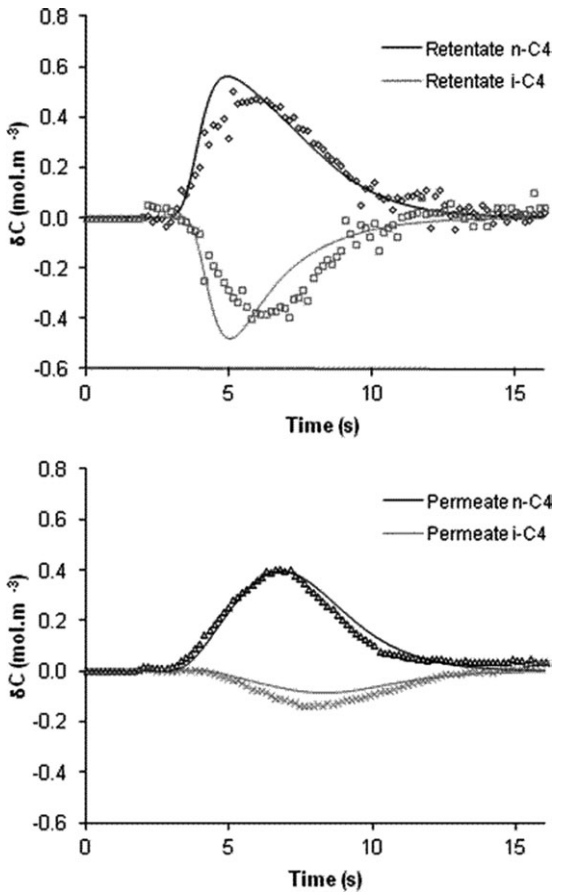


**Figure 10. *n*-Butane and isobutane outlet concentrations variations (M2 membrane, $T$ = 200°C, $P$ = 1 atm, $\overline{C}_{i,1} = \overline{C}_{o,1} = 5.15$ mol m$^{-3}$, $\overline{C}_{i,2} = \overline{C}_{o,2} = 5.15$ mol m$^{-3}$, pure *n*-butane pulse injection, continuous lines: simulations, points: experimental results).**

*Simulation of n-butane/isobutane mixtures experiments.* Other similar experiments have been performed and simulated by using the Langmuir model and zero loading diffusion coefficient estimated values. Two examples of results are represented in Figures 9 and 10 where the initial conditions have been varied. It can be seen that the accordance between the model and the experimental data is rather satisfactory.

## Discussion

In this section, we want to emphasize on the approach that we have adopted for the supported membrane characterization by using the time domain fitting of a dynamic model parameters. As a matter of fact, the supported zeolite membrane is not a system that is designed for characterization purposes but for its end-use so that its characterization is not facilitated. The zeolitic layer is grown within the porous support so that its thickness is not known. In order to perform its nondestructive characterization, one has to model the

complete system (the two gaseous phase flows, the support and the zeolitic layer) that leads to increase the number of parameters to estimate. Our approach is based on three main points. The first one is to design specific experiments to characterize the gaseous flows and the support contribution to the system response.[1,2] The second one is to perform linear experiments from an initial equilibrium point of the system. This approach is inspired from inverse chromatographic technique.[10,12] The advantage of this approach is to simplify the mathematical treatment of the estimation problem since a linear model has to be used (Fickian diffusion, linear equilibrium) for the parameter estimation. The third one is a deep analysis of the linearized model with respect to the estimation procedure. This deep analysis is based on the structural identifiability properties of the dynamic model that is used as they are defined within the framework of automatic control.[22] This analysis has lead us to propose a change of state variable for the adsorbent layer composition that preserves these properties by avoiding an over-parametrization of the linearized model. From this analysis, we have shown in the case of single adsorbate experiments that the equilibrium constant and the thickness of the adsorbent layer cannot be separated and we have proposed a specific experiment for the adsorbent layer thickness estimation.[1,2] When this change of state variable is used, we have also shown that the initial equilibrium conditions values of all the state variables of the system are measured that is a great advantage.

As far as the binary mixture experiments are concerned, we can propose some perspectives related to the structural analysis of the model. The structure of the linearized material balances within the zeolitic layer is not modified according to the fact the single file diffusion is assumed or not, only the definitions of the $\overline{\tau}_{z,jk}$ time constants are different. On the contrary, if the single file assumption is valid, the $\boldsymbol{B}$ matrix becomes diagonal. Conversely, provided that the four parameters contained in the $\boldsymbol{B}$ matrix can be estimated from transient experiments, the structural properties of this matrix can be used to check for the validity of the single file assumption. Finally, if the binary Langmuir model is used, the analysis of the matrix $\boldsymbol{\tau}^{-1}$ can lead to the design of specific experiments by a proper choice of $\overline{C}_1^*$ and $\overline{C}_2^*$. It is clear that such an analysis of the matrix $\boldsymbol{B}$ and $\boldsymbol{\tau}^{-1}$ can also be performed within the framework of other equilibrium models.

Whatever the mathematical analysis that can be made, one cannot neglect the experimental difficulties that can be encountered and the possible lack of sensitivity of some of the parameters that constitute the limit of the dynamical approach, particularly in the case of binary mixtures experiments. This difficulty has leaded us to abandon the blind estimation procedure that we have used in the single component case by introducing some *a priori* specific thermodynamic and kinetic assumptions.

## Conclusion

A transient permeation-based technique has been proposed previously for the nondestructive *in situ* physico-chemical and morphological characterization of zeolitic supported membranes and has been tested in the Henry domain for single adsorbates.[1,2,20,21] We have extended this approach to the characterization of these membranes above the Henry domain for single adsorbates as well as for binary mixtures. The experiments remain performed within the linear behavior domain of the system so that simple linear models for diffusion and equilibrium can be used to estimate the parameters in a way comparable to the inverse chromatography technique. In order to perform these parameter estimations, a deep analysis of the way the dynamic models are obtained is provided on the basis of the structural identifiability theory. Examples of the approach are provided by using *n*-butane and *n*-butane/isobutane mixtures as adsorbates and MFI-supported membranes provided by IFP Energies nouvelles. The results that we obtain are promising for future applications of our approach.

## Notation

$B = \frac{\kappa D}{e}$ = mass-transfer parameter, m s$^{-1}$
$\boldsymbol{B}$ = matrix of mass-transfer parameters, m s$^{-1}$
$C$ = gas phase concentration, mol m$^{-3}$
$D$ = diffusion coefficient, m$^2$ s$^{-1}$
$e$ = thickness, m
$k$ = mass-transfer coefficients, m s$^{-1}$
$N$ = diffusion flux, mol s$^{-1}$ m$^{-2}$
$P$ = pressure, Pa
$q$ = adsorbate concentration, mol m$^{-3}$
$R$ = ideal gas constant, J mol$^{-1}$ K$^{-1}$
$T$ = temperature, K
$u$ = velocity, m s$^{-1}$
$x$ = radial coordinate, m
$z$ = axial coordinate, m
$t$ = time, s

### *Greek letters*

$\varepsilon$ = macroporous support porosity
$\nabla$ = gradient operator
$\nabla\cdot$ = divergence operator
$\Delta$ = Laplace operator
$\beta$ = matrix for the flux expression in the binary case
$\gamma$ = matrix for the linearized equilibrium condition in the binary case
$\delta$ = small deviation of a variable from the equilibrium initial state
$\kappa$ = equilibrium constant
$\theta$ = adsorbate loading in the zeolitic layer
$\eta = \frac{x}{e}$ = dimensionless radial coordinate in the zeolitic layer
$\tau = \frac{e^2}{D}$ = diffusion time constant, s
$\boldsymbol{\tau}^{-1}$ = inverse of the diffusion time constant matrix, s$^{-1}$
$\mu$ = chemical potential, J mol$^{-1}$

### *Subscripts*

1 = *n*-butane
2 = isobutane
i = inner compartment
o = outer compartment
$j,k$ = components
s = macroporous support
z = zeolitic layer

### *Superscripts*

in = compartment inlet
out = compartment outlet
MS = Maxwell-Stefan
sat = saturation
$*$ = a gas phase at equilibrium with a given solid
$i - C_4$ = related to isobutane
$n - C_4$ = related to normal butane
$\overline{X}$ = value of $X$ at the initial equilibrium position

## Literature Cited


1. Courthial L, Baudot A, Tayakout-Fayolle M, Jallut C. A transient permeation-based method for composite zeolite membranes characterization. *AIChE J*. 2008;54:2527–2538.
2. Courthial L. Caractérisation des propriétés physico-chimiques et morphologiques des membranes zéolithes par mesure de perméation en régime transitoire. PhD thesis, Lyon University, 2007.

3. Chau C, Sicard M, Le Dred R. Membrane zéolithique de faible épaisseur, sa préparation et son utilisation en séparation. Eur. Patent EP 1369166 A1, 2003.
4. Chau C, Prevost I, Dalmon JA, Miachon S. Process for preparing supported zeolitic membranes by temperature-controlled crystallisation. US Patent 6,582,495 B2, 2003.
5. Chau C, Prevost I, Dalmon JA, Miachon S. Procédé de préparation de membranes zéolithiques supportées par cristallisation contrôlées en température. Eur. Patent EP 1230972 B1, 2006.
6. Gardner TQ, Lee JB, Noble RD, Falconer JL. Adsorption and diffusion properties of butanes in ZSM-5 zeolite membranes. *Ind Eng Chem Res*. 2002;41:4094–4105.
7. Gavalas GR. Diffusion in microporous membranes: measurements and modelling. *Ind Eng Chem Res*. 2008;47:5797–5811.
8. Hufton JR, Danner RP. Chromatographic study of alkanes in silicalite: equilibrium properties. *AIChE J*. 1993;39:954–961
9. Hufton JR, Danner RP. Chromatographic study of alkanes in silicalite: transport properties. *AIChE J*. 1993;39:962–974.
10. Tondeur D, Kabir H, Luo LA, Granger J. Multicomponent adsorption equilibria from impulse response chromatography. *Chem Eng Sci*. 1996;51:3781–3799.
11. Tayakout-Fayolle M, Jolimaitre E, Jallut C. Consequence of structural identifiability properties on state-model formulation for linear inverse chromatography. *Chem Eng Sci*. 2000;55:2945–2956.
12. Jolimaitre E, Tayakout-Fayolle M, Jallut C, Ragil K. Determination of mass transfer and thermodynamic properties of branched paraffins in silicalite by inverse chromatography technique. *Ind Eng Chem Res*. 2001;40:914–926.
13. Couenne F, Jallut C, Tayakout-Fayolle M. On minimal representation of heterogeneous mass transfer for simulation and parameter estimation: application to breakthrough curves exploitation. *Comput Chem Eng*. 2005;30:42–53.
14. Delgado JA, Nijhuis TA, Kapteijn F, Moulijn JA. Determination of adsorption and diffusion parameters in zeolites through a structured approach. *Chem Eng Sci*. 2004;59:2477–2487.
15. Sun MS, Talu O, Shah DB. Diffusion measurements through embedded zeolite crystals. *AIChE J*. 1996;42:3001–3007.
16. Bakker WJW, Kapteijn F, Poppe J, Moulijn JA. Permeation characteristics of a metal-supported silicalite-1 zeolite membrane. *J Membr Sci*. 1996;117:57–78.
17. Gardner TQ, Flores AI, Noble RD, Falconer JL. Transient measurements of adsorption and diffusion in H-ZSM-5 membranes. *AIChE J*. 2002;48:1155–1167.
18. Gardner TQ, Falconer JL, Noble RD, Zieverink MMP. Analysis of transient permeation fluxes into and out of membranes for adsorption measurements. *Chem Eng Sci*. 2003;58:2103–2112.
19. Gardner TQ, Falconer JL, Noble RD. Transient permeation of butane through ZSM-5 and ZSM-11 zeolite membranes. *AIChE J*. 2004;50:2816–2834.
20. Tayakout-Fayolle M, Jallut C, Lefevre F, Dalmon JA. *Application of transient methods to measurements of mass transfer parameters in zeolitic membranes. First European Congress on Chemical Engineering (ECCE1)*. Vol. 2, Florence, Italy, May 4–7, 1997: 1209–1212.
21. Courthial L, Baudot A, Jolimaitre E, Tayakout M, Jallut C. Moments method applied to the in-situ characterisation of normal butane mass transfer in MFI zeolite membranes. *Desalination*. 2006;193:215–223.
22. Walter E, Pronzato L. *Identification of Parametric Models from Experimental Data*. Berlin: Springer, 1997.
23. Sanchez J, Gijiu CL, Hynek V, Muntean O, Julbe A. The application of transient time-lag method for the diffusion coefficient estimation on zeolite composite membranes. *Sep Purif Technol*. 2001;25:467–474.
24. Krishna R. Multicomponent surface diffusion of adsorbed species: a description based on the generalized Maxwell-Stefan equations. *Chem Eng Sci*. 1990;45:1779–1791.
25. Krishna R, van den Broeke LJP. The Maxwell-Stefan description of mass transport across zeolite membranes. *Chem Eng J*. 1995;57:155–162.
26. Van de Graaf JM, Kapteijn F, Moulijn JA. Modeling permeation of binary mixtures through zeolite membranes. *AIChE J*. 1999;45: 497–511.
27. Kapteijn F, Moulijn JA, Krishna R. The generalized Maxwell-Stefan model for diffusion in zeolites: sorbates molecules with different saturation loadings. *Chem Eng Sci*. 2000;55:2923–2930.
28. Lee SC. Prediction of permeation behavior of $CO_2$ and $CH_4$ through silicalite-1 membranes in single-component or binary mixture systems using occupancy-dependent Maxwell-Stefan diffusivities. *J Membr Sci*. 2007;306:267–276.
29. Martinek JG, Gardner TQ, Noble RD, Falconer JL. Modeling transient permeation of binary mixtures through zeolite membranes. *Ind Eng Chem Res*. 2006;45:6032–6043.
30. Yu M, Falconer JL, Noble RD, Krishna R. Modeling transient permeation of polar organic mixtures through a MFI zeolite membrane using the Maxwell-Stefan equations. *J Membr Sci*. 2007;293:167–173.
31. Ruthven DM. *Principles of Adsorption and Adsorption Processes*. New-York: Wiley, 1984.
32. Lettat K, Jolimaitre E, Mélaz Tayakout M, Tondeur D. Liquid phase diffusion of branched alkanes in silicalite. *AIChE J*. 2011;57: 319–332.
33. Krishna R, van Baten JM, Describing mixture diffusion in microporous materials under conditions of pore saturation. *J Phys Chem C*. 2010;114:11557–11563.
34. Zhu W, van de Graaf JM, van den Broeke, Kapteijn F, Moulijn JA. TEOM: a unique technique of measuring adsorption properties. Light alkanes in silicalite-1. *Ind Eng Chem Res*. 1998;37:1934–1942.
35. Mori N, Tomita T. Separation of *n*-butane/iso-butane by self-supporting MFI membranes with various $SiO_2/Al_2O_3$. *Microporous Mesoporous Mater*. 2008;112:88–96.
36. Möller A, Pessoa Guimaraes A, Gläser R, Staudt R. Uptake-curves for the determination of diffusion coefficients and sorption equilibria for *n*-alkanes on zeolites. *Microporous Mesoporous Mater*. 2009; 125:23–29.
37. Song L, Sun Z, Duan L, Gui J, McDougall GS. Adsorption and diffusion properties of hydrocarbons in zeolites. *Microporous Mesoporous Mater*. 2007;104:115–128.
38. Miachon S, Landrivon E, Aouine M, Sun Y, Kumakiri I, Li Y, Patchova Prokopova O, Guilhaume N, Giroir-Fendler A, Mozzanega H, Dalmon JA. Nanocomposite MFI-alumina membranes via pore-plugging synthesis preparation and morphological characterization. *J Membr Sci*. 2006;281:228–238.
39. Aoki K, Tuan Vu A, Falconer JL, Noble RD. Gas permeation properties of ion-exchanged ZSM-5 zeolite membranes. *Microporous Mesoporous Mater*. 2000;39:485–492.
40. Jareman F, Hedlund J, Sterte J. Effects of aluminium content on the separation properties of MFI membranes. *Sep Purif Technol*. 2003;32:159–163.
41. Ciavarella P. Etude expérimentale et expérimentation du transport gazeux dans les membranes zéolithiques de type MFI. Application à la déshydrogénation de l'isobutane en réacteur catalytique à membrane. PhD thesis, Lyon university, 1999.
42. Noack M, Kölsch P, Seefeld V, Toussaint P, Georgi G, Caro J. Influence of the Si/Al ration on the permeation properties of MFI-membranes. *Microporous Mesoporous Mater*. 2005;79:329–337.
43. Kapteijn F, Bakker WJW, Zheng G, Moulijn JA. Temperature- and occupancy-dependent diffusion of *n*-butane through a silicalite-1 membrane. *Microporous Mater*. 1994;3:227–234.

## Appendix

If the binary Langmuir model with different saturation loadings for the adsorbates is assumed, that is to say $q_{z,j} = q_j^{sat} \frac{b_j c_j^*}{1+\sum_{k=1}^{2} b_k C_k^*}$, the $\overline{\gamma}$ matrix is given by

$$\overline{\gamma} = \begin{pmatrix} \left.\frac{\partial C_1^*}{\partial q_{z,1}}\right|_{C_1^*=\overline{C}_1^*, C_2^*=\overline{C}_2^*} & \left.\frac{\partial C_1^*}{\partial q_{z,2}}\right|_{C_1^*=\overline{C}_1^*, C_2^*=\overline{C}_2^*} \\ \left.\frac{\partial C_2^*}{\partial q_{z,1}}\right|_{C_1^*=\overline{C}_1^*, C_2^*=\overline{C}_2^*} & \left.\frac{\partial C_2^*}{\partial q_{z,2}}\right|_{C_1^*=\overline{C}_1^*, C_2^*=\overline{C}_2^*} \end{pmatrix} \tag{A1}$$

$$\overline{\gamma} = \begin{pmatrix} \frac{(1+b_1\overline{C}_1^*)\cdot(1+b_1\overline{C}_1^*+b_2\overline{C}_2^*)}{b_1 q_1^{sat}} & \frac{\overline{C}_1^*\cdot(1+b_1\overline{C}_1^*+b_2\overline{C}_2^*)}{q_2^{sat}} \\ \frac{\overline{C}_2^*\cdot(1+b_1\overline{C}_1^*+b_2\overline{C}_2^*)}{q_1^{sat}} & \frac{(1+b_2\overline{C}_2^*)\cdot(1+b_1\overline{C}_1^*+b_2\overline{C}_2^*)}{b_2 q_2^{sat}} \end{pmatrix}$$

In this case, one can verify that the following expression for the $\boldsymbol{B}$ matrix that is used for the boundary conditions expressions (18) is correct:

$$\boldsymbol{B} = \begin{pmatrix} \dfrac{q_1^{\mathrm{sat}} b_1 \left(\frac{b_1 \overline{C}_1^*}{D_{21}} + \frac{1}{D_2}\right)}{e_z \left(\frac{b_1 \overline{C}_1^*}{D_1 D_{21}} + \frac{b_2 \overline{C}_2^*}{D_2 D_{12}} + \frac{1}{D_1 D_2}\right)} & \dfrac{q_1^{\mathrm{sat}} b_1 b_2 \overline{C}_1^*}{e_z D_{12} \left(\frac{b_1 \overline{C}_1^*}{D_1 D_{21}} + \frac{b_2 \overline{C}_2^*}{D_2 D_{12}} + \frac{1}{D_1 D_2}\right)} \\ \dfrac{q_2^{\mathrm{sat}} b_1 b_2 \overline{C}_2^*}{e_z D_{21} \left(\frac{b_1 \overline{C}_1^*}{D_1 D_{21}} + \frac{b_2 \overline{C}_2^*}{D_2 D_{12}} + \frac{1}{D_1 D_2}\right)} & \dfrac{q_2^{\mathrm{sat}} b_2 \left(\frac{b_2 \overline{C}_2^*}{D_{12}} + \frac{1}{D_1}\right)}{e_z \left(\frac{b_1 \overline{C}_1^*}{D_1 D_{21}} + \frac{b_2 \overline{C}_2^*}{D_2 D_{12}} + \frac{1}{D_1 D_2}\right)} \end{pmatrix} \tag{A2}$$

As far as the elements of the $\boldsymbol{\tau}^{-1} = \begin{pmatrix} \frac{1}{\overline{\tau}_{z,11}} & \frac{1}{\overline{\tau}_{z,12}} \\ \frac{1}{\overline{\tau}_{z,21}} & \frac{1}{\overline{\tau}_{z,2}} \end{pmatrix}$ matrix are concerned, the following expressions are obtained accordingly:

$$\begin{aligned}
\frac{1}{\overline{\tau}_{z,11}} &= \frac{(1 + b_1 \overline{C}_1^* + b_2 \overline{C}_2^*)}{e_z^2 \left(\frac{b_1 \overline{C}_1^*}{D_1 D_{21}} + \frac{b_2 \overline{C}_2^*}{D_2 D_{12}} + \frac{1}{D_1 D_2}\right)} \left((1 + b_1 \overline{C}_1^*) \left(\frac{b_1 \overline{C}_1^*}{D_{21}} + \frac{1}{D_2}\right) + \frac{b_1 b_2 \overline{C}_1^* \overline{C}_2^*}{D_{21}}\right) \\
\frac{1}{\overline{\tau}_{z,12}} &= \frac{(1 + b_1 \overline{C}_1^* + b_2 \overline{C}_2^*) b_2 \overline{C}_1^*}{e_z^2 \left(\frac{b_1 \overline{C}_1^*}{D_1 D_{21}} + \frac{b_2 \overline{C}_2^*}{D_2 D_{12}} + \frac{1}{D_1 D_2}\right)} \left(\frac{(1 + b_1 \overline{C}_1^*)}{D_{12}} + \frac{b_2 \overline{C}_2^*}{D_{12}} + \frac{1}{D_1}\right) \\
\frac{1}{\overline{\tau}_{z,21}} &= \frac{(1 + b_1 \overline{C}_1^* + b_2 \overline{C}_2^*) b_1 \overline{C}_2^*}{e_z^2 \left(\frac{b_1 \overline{C}_1^*}{D_1 D_{21}} + \frac{b_2 \overline{C}_2^*}{D_2 D_{12}} + \frac{1}{D_1 D_2}\right)} \left(\frac{(1 + b_2 \overline{C}_2^*)}{D_{21}} + \frac{b_1 \overline{C}_1^*}{D_{21}} + \frac{1}{D_2}\right) \\
\frac{1}{\overline{\tau}_{z,22}} &= \frac{(1 + b_1 \overline{C}_1^* + b_2 \overline{C}_2^*)}{e_z^2 \left(\frac{b_1 \overline{C}_1^*}{D_1 D_{21}} + \frac{b_2 \overline{C}_2^*}{D_2 D_{12}} + \frac{1}{D_1 D_2}\right)} \left((1 + b_2 \overline{C}_2^*) \left(\frac{b_2 \overline{C}_2^*}{D_{12}} + \frac{1}{D_1}\right) + \frac{b_1 b_2 \overline{C}_1^* \overline{C}_2^*}{D_{21}}\right)
\end{aligned} \tag{A3}$$

*Manuscript received Jan. 10, 2012, and revision received May 18, 2012.*